

More than just exosomes: distinct *Leishmania infantum* extracellular products potentiate the establishment of infection

Begoña Pérez-Cabezas, Nuno Santarém, Pedro Cecílio, Cátia Silva, Ricardo Silvestre, José A. M. Catita & Anabela Cordeiro da Silva

To cite this article: Begoña Pérez-Cabezas, Nuno Santarém, Pedro Cecílio, Cátia Silva, Ricardo Silvestre, José A. M. Catita & Anabela Cordeiro da Silva (2018) More than just exosomes: distinct *Leishmania infantum* extracellular products potentiate the establishment of infection, Journal of Extracellular Vesicles, 7:1, 1541708, DOI: [10.1080/20013078.2018.1541708](https://doi.org/10.1080/20013078.2018.1541708)

To link to this article: <https://doi.org/10.1080/20013078.2018.1541708>



© 2018 The Author(s). Published by Informa UK Limited, trading as Taylor & Francis Group on behalf of The International Society for Extracellular Vesicles.



Published online: 08 Nov 2018.



Submit your article to this journal [↗](#)



Article views: 455



View Crossmark data [↗](#)

RESEARCH ARTICLE



More than just exosomes: distinct *Leishmania infantum* extracellular products potentiate the establishment of infection

Begoña Pérez-Cabezas^{a,b*}, Nuno Santarém^{a,b*}, Pedro Cecílio^{a,b}, Cátia Silva^{a,b}, Ricardo Silvestre^c, José A. M. Catita^{d,e} and Anabela Cordeiro da Silva^{a,b,f*}

^aInstituto de Investigação e Inovação em Saúde, Universidade do Porto, Porto, Portugal; ^bParasite Disease Group, Instituto de Biologia Molecular e Celular, Universidade do Porto, Porto, Portugal; ^cMicrobiology and Infection Research Domain, Life and Health Sciences Research Institute (ICVS), School of Medicine, University of Minho, Braga, Portugal; ^dFP-ENAS Research Unit, UFP Energy, Environment and Health Research Unit, CEBIMED, Biomedical Research Centre, Fernando Pessoa University, Porto, Portugal; ^eParalab, SA, Valbom, Portugal; ^fDepartamento de Ciências Biológicas, Faculdade de Farmácia da Universidade do Porto, Porto, Portugal

ABSTRACT

The use of secretion pathways for effector molecule delivery by microorganisms is a trademark of pathogenesis. *Leishmania* extracellular vesicles (EVs) were shown to have significant immunomodulatory potential. Still, they will act in conjunction with other released parasite-derived products that might modify the EVs effects. Notwithstanding, the immunomodulatory properties of these non-vesicular components and their influence in the infectious process remains unknown. To address this, we explored both in vitro and in vivo the immunomodulatory potential of promastigotes extracellular material (EXO), obtained as a whole or separated in two different fractions: EVs or vesicle depleted EXO (VDE). Using an air pouch model, we observed that EVs and VDE induced a dose-dependent cell recruitment profile different from the one obtained with parasites, attracting significantly fewer neutrophils and more dendritic cells (DCs). Additionally, when we co-inoculated parasites with extracellular products a drop in cell recruitment was observed. Moreover, in vitro, while VDE (but not EVs) downregulated the expression of DCs and macrophages activation markers, both products were able to diminish the responsiveness of these cells to LPS. Finally, the presence of *Leishmania infantum* extracellular products in the inoculum promoted a dose-dependent infection potentiation in vivo, highlighting their relevance for the infectious process. In conclusion, our data demonstrate that EVs are not the only relevant players among the parasite exogenous products. This, together with the dose-dependency observed, opens new avenues to the comprehension of *Leishmania* infectious process. The approach presented here should be exploited to revisit existing data and considered for future studies in other infection models.

ARTICLE HISTORY

Received 18 June 2018
Revised 21 September 2018
Accepted 23 October 2018

KEYWORDS



Leishmania; extracellular vesicles; exosomes; air pouch; immunomodulation; macrophages; dendritic cells; infection

Introduction

Microorganisms influence and are influenced by their surroundings in a dynamic process, representing the main driving force in evolution. The interactions between the immune system and microbial pathogens take this to the extreme in a millennia-old struggle for survival. Protozoan parasites of the genus *Leishmania* are an excellent example. Remarkably, amastigotes, the parasite intracellular form, evolved to survive and proliferate in the inhospitable environment of the macrophage phagolysosome [1]. This remarkable adaptation ultimately contributes to *Leishmania* pathogenicity, being these protozoa responsible for a spectrum of diseases designated as leishmaniasis. Annually an estimated 1.3 million new cases and 20 000 to 30 000 deaths are associated with these diseases [2]. The absence of human vaccines to prevent

leishmaniasis [3] and the risks associated with conventional therapies urge for a better understanding of the infectious process.

The comprehension of the immune response associated with *Leishmania* infection is a fast evolving field comprising different parasite species and infection models [4]. It is accepted that infection success depends on the parasite capacity to manipulate the immune system during the first stages of the infection [5]. *Leishmania* promastigotes are transmitted during the blood-feeding process of infected sand flies. In this context, components of the initial inoculum such as the sand fly saliva and parasite-derived products, like promastigote secretory gel (PSG), have been evaluated for their possible roles in the establishment of infection [6,7]. More recently also *Leishmania* derived extracellular vesicles (EVs) have

CONTACT Anabela Cordeiro da Silva  cordeiro@ibmc.up.pt  Instituto de Investigação e Inovação em Saúde, Universidade do Porto, Porto, Portugal

*These authors contributed equally to this work.

© 2018 The Author(s). Published by Informa UK Limited, trading as Taylor & Francis Group on behalf of The International Society for Extracellular Vesicles. This is an Open Access article distributed under the terms of the Creative Commons Attribution-NonCommercial License (<http://creativecommons.org/licenses/by-nc/4.0/>), which permits unrestricted non-commercial use, distribution, and reproduction in any medium, provided the original work is properly cited.

been recovered from sand fly midguts and were presented as possible players during the initial steps of infection [8]. These EVs were found similar in composition to in vitro recovered EVs validating the in vitro approaches as a valuable source of biologically relevant EVs [8]. However, depending on the approach used to produce the conditioned media (continuous vs. discontinuous) from which the EVs are recovered, different proteomic profiles are obtained [9]. Significantly, our group reported previously that only in continuous culture conditions the EVs from stationary parasites are dominated by GP63 [9], whose immunomodulatory properties enable direct modulation of host signalling [10–13]. This virulence factor has been a focus of several *Leishmania* EVs studies [14,15]. Additionally, other known immunomodulatory proteins like aldolase, elongation factor 1- α and kinetoplastid membrane 11 were also detected by us and others in EVs preparations [9,16–18].

EVs are often treated as isolated entities and the contribution of other secreted components is not accounted for in the many studies published over the years [19,20]. *Leishmania* promastigotes derived EVs are no exception; they are part of the extracellular products released by the parasite while residing inside the sand fly. Therefore, it is important to understand if reported *Leishmania* EVs immunological properties are maintained in the context of other extracellular products. The *Leishmania* extracellular material (EXO) can be separated physically into two distinct components: EVs and vesicle depleted EXO (VDE) [9]. The relative abundance and protein composition of the VDE and EVs were previously characterized by us [9], and are different, suggesting that they might have distinct immunomodulatory potential. Herein we compare the impact of distinct EXO amounts and its fractions, EVs and VDE, in cell recruitment, antigen presenting cells responsiveness (DCs and macrophages) and infection outcome both in vitro and in vivo. Ultimately, the characterized immunomodulatory properties of each fraction translate into a dose-dependent potentiation of infection, which can be translated to the natural infection, considering the secretome as a whole.

Materials and methods

Ethics statement

All animal experiments were carried out in accordance with the IBMC/INEB Animal Ethics Committees and the Portuguese National Authorities for Animal Health guidelines, according to the statements on the Directive 2010/63/EU of the European Parliament and of the

Council. BPC, NS and ACS have an accreditation for animal research given by the Portuguese Veterinary Direction (Ministerial Directive 1005/92).

Leishmania infantum culture

A cloned line of virulent *Leishmania infantum* (MHOM/MA/67/ITMAP-263) freshly recovered from BALB/c mice was used for a total of 10 passages. Promastigotes were routinely maintained at 26°C in standard RPMI 1640 medium supplemented with 10% heat-inactivated Fetal Calf Serum (FCS; Biowest, Nuaille, France), 2 mM L-glutamine, 100 U/ml penicillin, 100 µg/ml streptomycin and 20 mM HEPES buffer, all products from Lonza (Basel, Switzerland). For extracellular products obtention, parasites were previously adapted and then sub-cultured (26°C) for 4 days (stationary phase [21]) in serum-free culture media – cRPMI [RPMI base complemented with 10% SDM-79 base and 2.5 µg/ml of hemin (Sigma-Aldrich, St. Louis, MO, USA)] – that we previously developed and validated for exoproteome studies [9,21]. All maintenance cultures were grown with a starting inoculum of 10⁶ parasites/ml.

Extracellular products recovery

Promastigotes were cultured at an initial concentration of 2 × 10⁶ parasites/ml in cRPMI. After 4 days the parasites were removed by centrifugation at 1800 g during 10 min at 4°C. The recovered conditioned media (always on ice from this point on) was passed through a 0.45 µm filter to remove any remaining parasites and concentrated at 4000 g and 8°C using 100 kDa Amicon® Ultra Centrifuge Filters, Ultracol® (Merck Millipore, Billerica, MA, USA) until the residual volume was less than 500 µl. The full volume of the 100 kDa concentrate was dialyzed twice with 15 ml of PBS until a residual volume of less than 500 µl. The flow-through was stored for VDE recovery. For EXO the process was similar, but using 3 kDa Amicon® Ultra Centrifuge Filters, Ultracol®. The 100 kDa fraction containing the EVs was then transferred to Ultra-Clear™ centrifuge tubes for centrifugation in the Beckman Coulter, optima L-80 XP ultracentrifuge with a SW41 rotor for 14 h at 100 000 g and 4°C. The following day the supernatant was recovered without disturbing the pellet, for VDE concentration. The pellet was suspended and dialyzed twice with 15 ml of PBS using the 100 kDa columns mentioned above until a final volume of less than 500 µl was reached. For the VDE, the process began by centrifuging the stored filtrate from the 100 kDa filtrations, together with the

supernatant from the ultracentrifugation through 3 kDa Amicon® Ultra Centrifuge Filters, Ultracol®, followed by two consecutive dialyses with 15 ml PBS until the residual volume was less than 500 µl. All the volumes of the preparations were then adjusted to the volume containing the material released by 10^7 parasites/µl that we represent in the manuscript as “e⁷”. In the assays e⁶ (0.1 µl), e⁷ (1 µl), e⁸ (10 µl) and e⁹ (100 µl) were used. For the biological assays, all stimuli were used within the 24 h after purification. Proteomic studies of similarly obtained preparations were already performed and analysed (EV TRACK ID: EV180055) [9].

Transmission electron microscopy

The EXO, EVs and VDE were observed by Transmission electron microscopy (TEM). For this, equivalent amounts of the recovered preparations were placed onto Formvar/Carbon-coated copper grids and stained with an aqueous solution of 3% uranyl acetate (Sigma-Aldrich, St. Louis, MO, USA) for 10 min. Samples were viewed in a Zeiss model EM 10C electron microscope.

Extracellular vesicles size determination

The average EVs size determination was performed using TEM, dynamic light scattering (DLS) and Nanoparticle Tracking Analysis (NTA). The particle diameter from the TEM images was determined using the ImageJ software package version 1.43u. A total number of 1000 particles from images from 5 different experiments were used for the size estimation. Concerning the Z average size and the polydispersity index determinations, they were performed using a Zetasizer Nano ZS (Malvern Instruments, Malvern, UK) with a detection angle of 173°. Measurements were made in triplicate at 25°C and analysed with the Zetasizer series software – version 7.01. For NTA the determinations were performed using a NanoSight NS300 (Malvern Instruments, Malvern, UK) with the software version NTA 3.0.

EV-TRACK

We have submitted all relevant data of our experiments to the EV-TRACK knowledgebase (EV-TRACK ID: EV180058) [22].

Mice

Female BALB/c mice were purchased from Charles River Laboratories (France) and maintained under

laboratory conditions at IBMC Animal Facilities, in sterile IVC cabinets, with food and water available *ad libitum*. All animals used in experiments were aged from six to eight weeks.

Air pouch model and in vivo cellular recruitment experiments

Air pouches were raised on the dorsum of isoflurane (Piramal healthcare, Northumberland, UK) anesthetized BALB/c mice by s.c. injection of 3 ml sterile air on day 0, and 2 ml on day 3, as previously described [23,24]. On day 6, the formed synovial air pouch cavities received different stimuli, diluted in endotoxin-free sterile PBS (Gibco, Gaithersburg, MD, USA) to a final volume of 1 ml. 1×10^6 , 1×10^7 and 1×10^8 *L. infantum* promastigotes, or the EXO, VDE and EVs produced by the same number of parasites were used (final concentration of 10^{6-8} /ml). Furthermore, 1×10^6 *L. infantum* promastigotes were injected together with e⁷ EXO, VDE or EVs. Control mice received only PBS (negative control) or 20 µg LPS (positive control). Six hours after intra-pouch inoculation, corresponding to the infiltration peak [25] animals were euthanized, then the air pouches were aseptically exposed, and their contents were thoroughly washed with a total of 3 ml of endotoxin-free, ice-cold PBS, to collect the recruited cells. The recovered cells were counted using a Neubauer chamber and the myeloid cell populations were resolved by flow cytometry. Additionally, the activation status of exudate DCs was also assessed by flow cytometry 24 h after the injection.

Bone marrow-derived macrophages and DCs generation

Bone marrow precursors were recovered with RPMI 1640 medium after flushing femurs and tibias of BALB/c mice. Cells were washed and counted using a Neubauer chamber. Bone marrow-derived DCs (BMDC) were obtained, based on a protocol previously described [26], by seeding 6×10^6 bone marrow cells in 25 ml of complete RPMI supplemented with 50 µM 2-mercaptoethanol (Sigma-Aldrich, St. Louis, MO, USA) and 10% of J558 cell conditioned medium (DC medium). Cells were cultured at 37°C and 5% CO₂ for 3 days. After, the same amount of DC medium was added to each flask. At day 6, half of the culture supernatant was replaced with the same amount of fresh DC medium. At day 8, cells were recovered, counted and finally plated in 96-well culture plates at a final amount of 1×10^5 cells/well in 200 µl of DC medium. CD11c⁺ MHC-II⁺ cells, considered as BMDC and determined by flow cytometry, represented more

than 75% of the culture. Bone marrow-derived macrophages (BMMØ) were obtained from non-adhered bone marrow cells collected after an initial overnight incubation (37°C and 5% CO₂) in complete Dulbecco's modified Eagle's medium (DMEM) (Lonza, Switzerland) as previously described [27]. Non-adherent cells were recovered, counted and distributed in 96 well culture plates at 1×10^5 cells/well in 100 µl of complete DMEM supplemented with 5% of L-929 cell conditioned medium (LCCM). At day 3 of culture, 100 µl of DMEM + 5% LCCM were added per well. Half of the media was renewed on day 6. Macrophages were used at day 8 of culture.

In vitro BMMØ and BMDCs stimulation experiments

Fully differentiated BMMØ or BMDCs were cultured during 48 h with increasing amounts of EXO, VDE or EVs in a way to assess dose dependency. The extracellular materials used in all experiments were produced by 6×10^6 (minimum amount to observe an in vitro effect after 48 h of culture with BMDC), 6×10^7 , and 1.2×10^8 parasites – $6e^6$, $6e^7$ and $1.2e^8$, respectively. For re-stimulation experiments, LPS (1 µg/ml) or PolyI:C (10 µM) (both from Sigma-Aldrich, St. Louis, MO, USA) were added after 24 h of culture and cells were then maintained for an additional 24 h. As a control, BMDCs were infected with increasing amounts of *L. infantum* promastigotes – DC:*L. infantum* ratios of 1:0.5, 1:1, 1:2, 1:5, 1:10 and 1:20. After 4 h, cells were extensively washed and the culture maintained for 48 h. The control cells were left unstimulated during the 48 culture hours. Cells were then washed, recovered and stained for analysis of activation markers expression by flow cytometry.

Labelled monoclonal antibodies and flow cytometry

The anti-mouse monoclonal antibodies used to perform this study were all purchased from BioLegend (San Diego, CA, USA) unless stated otherwise. FITC α-MHC-II (I-A/I-E); PE α-Siglec-F (BD Biosciences (BD), East Rutherford, NJ, USA), PE α-CD40; PerCP-Cy5.5 α-Ly6C; PE-Cy7 α-CD11b; APC-Cy7 α-CD11c; APC α-Ly6C; BV510 α-CD86; Pacific Blue™ Ly6G. Cell viability was assessed (in vitro experiments) using 7-aminol-actinomycin D (7-AAD, BioLegend). Surface staining was performed during 30 min in flow cytometry buffer (PBS + 0.5 % BSA) at 4°C in darkness. All the antibodies were used at a 1:100 dilution. Cells were then washed and resuspended in 150 µl flow cytometry buffer [28]. Flow cytometric acquisitions were performed in a FACSCanto™ II (BD) and

analysed with FlowJo software v10 (TreeStar, Ashland, OR, USA). Myeloid cell populations present in air pouch exudates were resolved as: Eosinophils (Siglec-F⁺/SSC-H^{int/high}), Neutrophils (CD11b^{high}/Ly6G^{high}), Dendritic Cells (CD11c⁺/MHC-II^{int/high}) and Macrophages/monocytes (CD11b⁺/Ly6C⁺/Ly6G⁻/CD11c⁻/Siglec-F⁻) [29]. In some air pouch experiments, the expression of CD40 and MHC-II was studied on DCs. For in vitro experiments, 7AAD⁺ dead cells were excluded before analysis of CD40, MHC-II and CD86 surface expression measured by Mean Fluorescence Intensity (MFI).

In vitro infection of BMMØ and BMDCs and cytospin

1×10^6 *L. infantum* promastigotes with or without $6e^6$ or $1.2e^8$ amounts of EXO, VDE or EVs were added to 1×10^5 fully differentiated BMMØ or BMDCs (MOI of 10). Infected non-stimulated cells were used as controls. Cells were gently washed after 4 h of infection (37°C and 5% CO₂) and immediately recovered, or cultured for 24 or 48 h and recovered afterward. Recovered cells were subjected to cytospin for 5 min at 1000 rpm (Shandon CytoSpin II, GMI, Ramsey, MN, USA), and fixed with 2% paraformaldehyde for 20 min at RT. Afterwards, the preparations were stained using the Giemsa method, as previously described [30]. Briefly, slides were immersed for 45 s in Hemacolor reagent 1, and for 45 more seconds in Hemacolor reagent 2 (Merk Millipore, Billerica, MA, USA). Finally, preparations were thoroughly washed with distilled water, air dried and observed by optical microscopy (100x magnification). The percentage of infected cells was determined by counting 200 consecutive cells, both infected and non-infected, in 3 different areas of the same preparation. The number of parasites within cells was defined counting 100 different infected cells.

In vivo infections

A low virulence experimental model was used. Distinct groups of mice were infected intraperitoneally with 1×10^7 *L. infantum* promastigotes together with increasing amounts (e^7 , e^8 or e^9) of either EXO, VDE or EVs. Control animals were infected only with 1×10^7 *L. infantum* promastigotes. The final infective volumes were adjusted to 100 µl with endotoxin-free sterile PBS. Fifteen days post-infection, animals were euthanized, and their spleens and livers were aseptically collected and homogenized using Falcon®100 µm Cell Strainers (Corning Life Sciences, Tewksbury, MA, USA) and manual Potter-Elvehjem tissue homogenizers, respectively. Spleen and liver parasite

burdens were then assessed by the limit dilution method starting with 3 mg and 15 mg of organ, respectively, as previously described [31].

Statistical analysis

Results are expressed as the mean \pm SEM unless otherwise stated. Some data are presented as relative values to the relevant control situation. Statistical comparisons were performed using the unpaired *t*-test or the one-sample *t*-test for comparison of relative values. Analyses were performed using the GraphPad Prism v6.01 software (GraphPad Software, San Diego, CA, USA). A *p*-value ≤ 0.05 was considered significant. To simplify, only the detected significant differences are graphically represented in the different figures (both main and supplementary).

Results

Physical characterization of the extracellular products

In a previous study, we used a combination of concentration and ultracentrifugation steps to recover VDE and EVs for proteomic studies, comparing logarithmic with stationary parasites [9]. Importantly, parasites were grown in a simple serum-free media, to warrant that all the recovered materials were of parasite origin

[9,21]. Here we used the same technical approach to recover extracellular products from stationary parasites. The obtained EXO contained mostly morphologically undefined material with a few scattered EVs (Figure 1(a)). The VDE was composed predominantly of undefined products while EVs preparations contained mainly cup-shaped structures. The preparations protein contents were more similar between VDE and EXO than between EVs and EXO (S1 Fig). To further characterize the EVs preparations, size, particle number and flotation density were determined (Figure 1(b), S2 Fig). The EVs preparations contained particles with average sizes between 77 and 130 nm depending on the method used to measure them (Figure 1(b)). Although almost 50% of the EVs had a predicted size between 40 and 70 nm (determined by TEM), the global size distribution ranged from 10 to 200 nm (Figure 1(c)). The average particle concentration, as determined by NTA, was $1.84 \times 10^{12}/\text{ml}$. The EVs flotation density and hydrodynamic average size (determined by DLS) enabled the recovery of distinct fractions containing EVs with characteristic sizes and densities (S2 Fig). Considering the traditional classifications proposed for EVs, we found particles with density and size similar to exosomes, exosome-like particles and apoptotic bodies (S2 Fig) [32]. The process also enabled the recovery of small-sized RNAs in the EVs preparations that were protected from RNase treatment (S3 Fig).

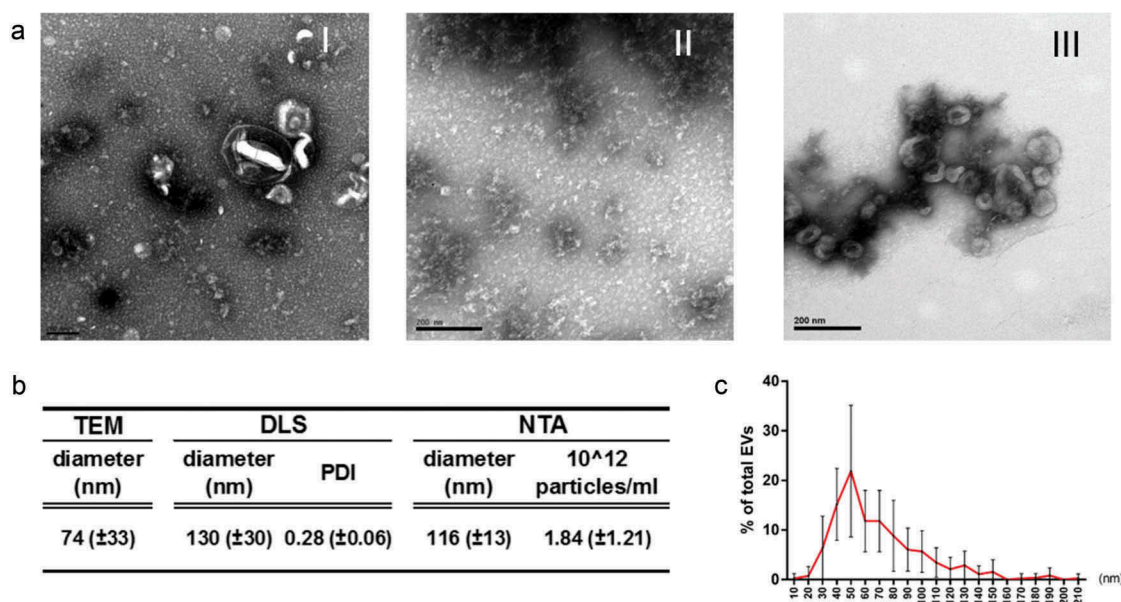


Figure 1. EVs and VDE represent distinct aspects of the total EXO. Representative TEM images of equivalent amounts of EXO (I) and the respective fractions VDE (II) and EVs (III) stained with acetate uracil (a). Average diameter of EVs preparations determined by TEM, DLS and NTA (b). Polydispersity index (PDI) and average particle number/ml of the preparations are also represented (b). Average dispersion of particle size (diameter) in the EVs population determined by direct measurement from TEM preparations (c). All the data are presented as average \pm SD from a minimum of 5 independent preparations.

Extracellular products released by *L. infantum* induce a differential and dose-dependent cell recruitment

Several authors reported early neutrophil recruitment in air pouch models associated with *Leishmania* promastigotes and their EVs [25,33]. To evaluate if EVs-induced recruitment is specific or a general characteristic of promastigotes and their EXO we evaluated cell recruitment in BALB/c air pouches in response to three doses of EXO, VDE, EVs and *L. infantum* promastigotes. Six hours after the inoculation, the air pouch cellular content was characterized by flow cytometry (Figure 2). A dose-dependent cell recruitment was induced by live parasites and all the tested stimuli (Figure 2(a)). When less than 1000 parasites/ μl (10^6 inoculum) were injected no significant recruitment was observed. The highest dose of EXO, VDE and EVs significantly increased the cell numbers in the air pouch (at least $p \leq 0.01$), while VDE at the e^6 dose significantly diminished the total cell numbers when compared with PBS (Figure 2(a); $p \leq 0.05$). Considering specific cellular populations, neutrophils increased for the higher doses of all tested stimuli (Figure 2(b); at least $p \leq 0.01$). Parasites induced a concentration-dependent neutrophil recruitment. On the contrary, e^6 and e^7 EVs and e^6 VDE significantly decreased the presence of neutrophils in the air pouch ($p \leq 0.05$). The macrophage/monocyte numbers were significantly increased, when compared to PBS, at the highest stimuli concentration tested (at least $p \leq 0.01$). A significant increase in the macrophage/monocyte recruitment was also observed for the e^7 and e^8 parasite doses (at least $p \leq 0.05$). After parasites administration eosinophils remained mostly unchanged. EXO and VDE at the highest concentration tested increased the presence of eosinophils in the air pouch (at least $p \leq 0.05$), while VDE at the lowest dose significantly decreased their recruitment ($p \leq 0.05$). Finally, the abundance of DCs was specific for VDE and EVs (Figure 2(b), S4A Fig, at least $p \leq 0.05$). The phenotype of recruited DCs by the e^8 dose was also analysed 24 h after inoculation. The expression patterns of surface costimulatory protein CD40 and the antigen presenting molecule MHC-II were overall similar to the PBS and distinct from LPS inoculation (S4 Fig), suggesting that these cells are non-activated at the inoculation site.

As a consequence of the cellular abundances induced by the stimuli, distinct cellular environments were evident (Figure 2(c)). At the highest concentration tested the parasites induce a cellular environment that is indistinguishable from LPS, with neutrophils and eosinophils

constituting more than 95% of the cells present in the air pouch. The reduction in parasite number led to distinct cellular environments with a lesser representation of neutrophils. Although the EXO also induced a cellular environment dominated by neutrophils, 20% of the cells present were macrophages/monocytes and DCs. The VDE presented a cellular environment that was similar for the three concentrations tested while EVs increased representation of neutrophils for the e^8 concentration (Figure 2(c)).

***L. infantum* extracellular material modifies the cellular recruitment induced by the parasite**

Considering that exposition to extracellular products induced distinct cellular recruitment profiles, their influence on the intrinsic recruitment induced by the parasites was investigated. When e^7 parasites together with e^7 EXO or its fractions were used (the doses with an intermediate effect), the individual cellular recruitment observed was always inferior in comparison to the one induced only by parasites (S5A Fig), although without statistical significance. Furthermore, with these experimental conditions, no changes were detected in the overall profile of the cell populations recruited to the air pouches (S5B Fig). Interestingly, when reducing the parasite number to 10^6 , the presence of extracellular products significantly decreased the recruitment induced by parasites (Figure 3(a); $p \leq 0.01$). In these conditions, and particularly looking at the effect of the separated extracellular materials (EVs and VDE) on the parasite-induced cell recruitment, a tendential reduction in the proportion of neutrophils (average of 30% to 20%) and a slight increase in the cumulative frequency of DCs and macrophages was observed (average of 20% to 30%) (Figure 3(b)), which aligns with the results described above for the cell recruitment induced by the extracellular products (Figure 2(b)). Therefore, the presence of extracellular products in the infectious inoculum can alter the cellular environment induced by the parasite alone (Figure 3(a-c)).

***L. infantum* extracellular products do not activate DCs and macrophages and hamper their responses to TLR ligands**

To evaluate the direct effect of extracellular products on DCs and macrophages, cells differentially recruited by the presence of VDE and EVs, bone marrow-derived DCs (BMDC) and macrophages (BMM \emptyset) were cultured in vitro with increasing amounts of EXO, VDE and EVs. After 48 h, the expression of

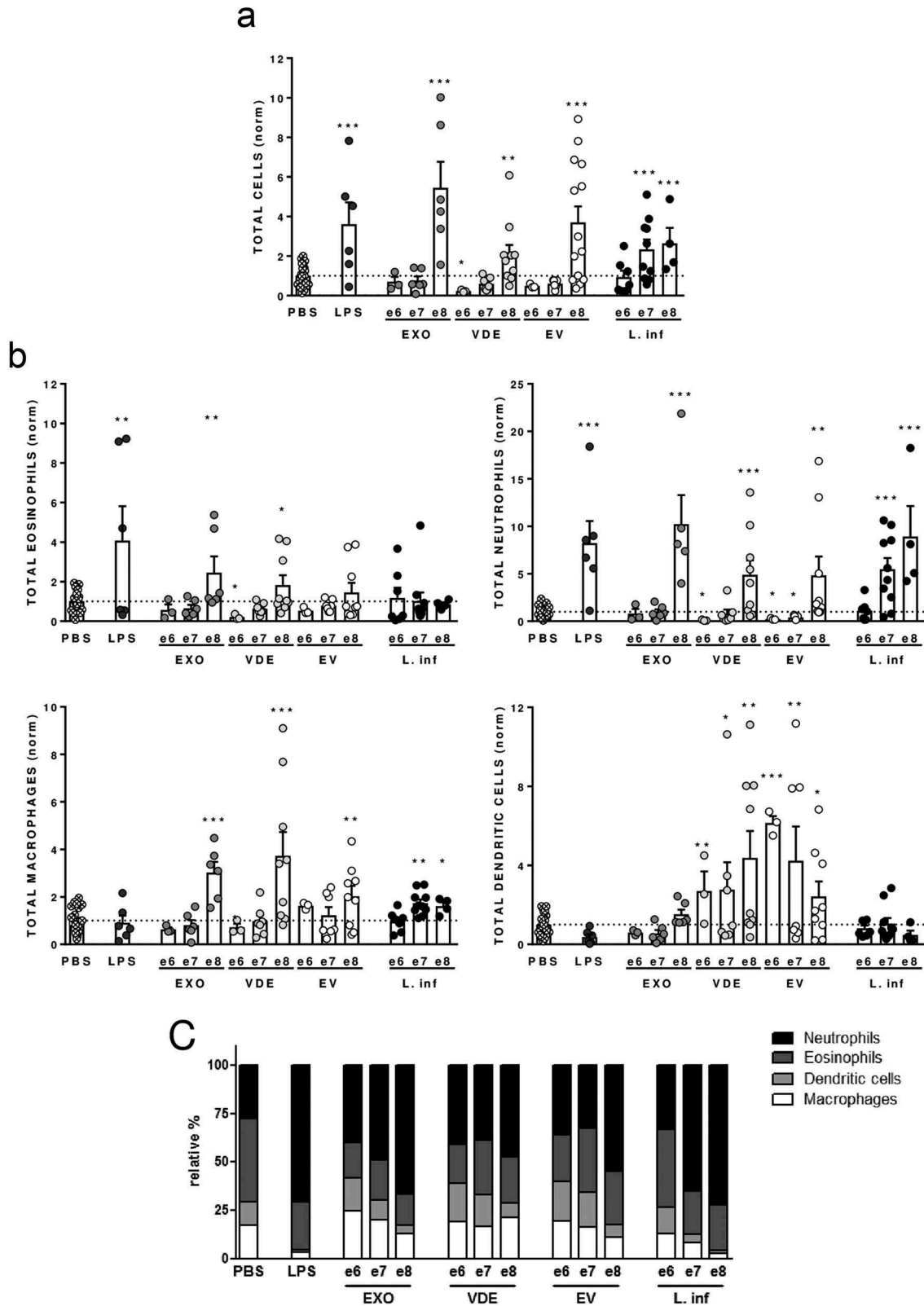


Figure 2. *Leishmania infantum* extracellular products promote a dose-dependent differential cell recruitment. Relative number of total cells (a), eosinophils, neutrophils, macrophages/monocytes and dendritic cells (normalized against the PBS recruitment) (b) and relative cellular abundance (c) in mice pre-formed air pouches 6 h after the injection of PBS (crossed dots), LPS (dark grey dots), 10^6 , 10^7 and 10^8 *L. infantum* promastigotes (black dots) or the EXO (medium grey dots), VDE (light grey dots) and EVs (white dots) produced by the same number of parasites (e^6 , e^7 and e^8). Cells were quantified using a Neubauer chamber and the phenotype analysed by flow cytometry. Each dot represents an animal. Bars represent the average (\pm SEM) obtained from the animals studied in three different experiments. One-sample *t*-test was used to assess statistical significances comparing to the PBS control group. Significant differences are highlighted in the figure: * $p \leq 0.05$, ** $p \leq 0.01$, *** $p \leq 0.001$.

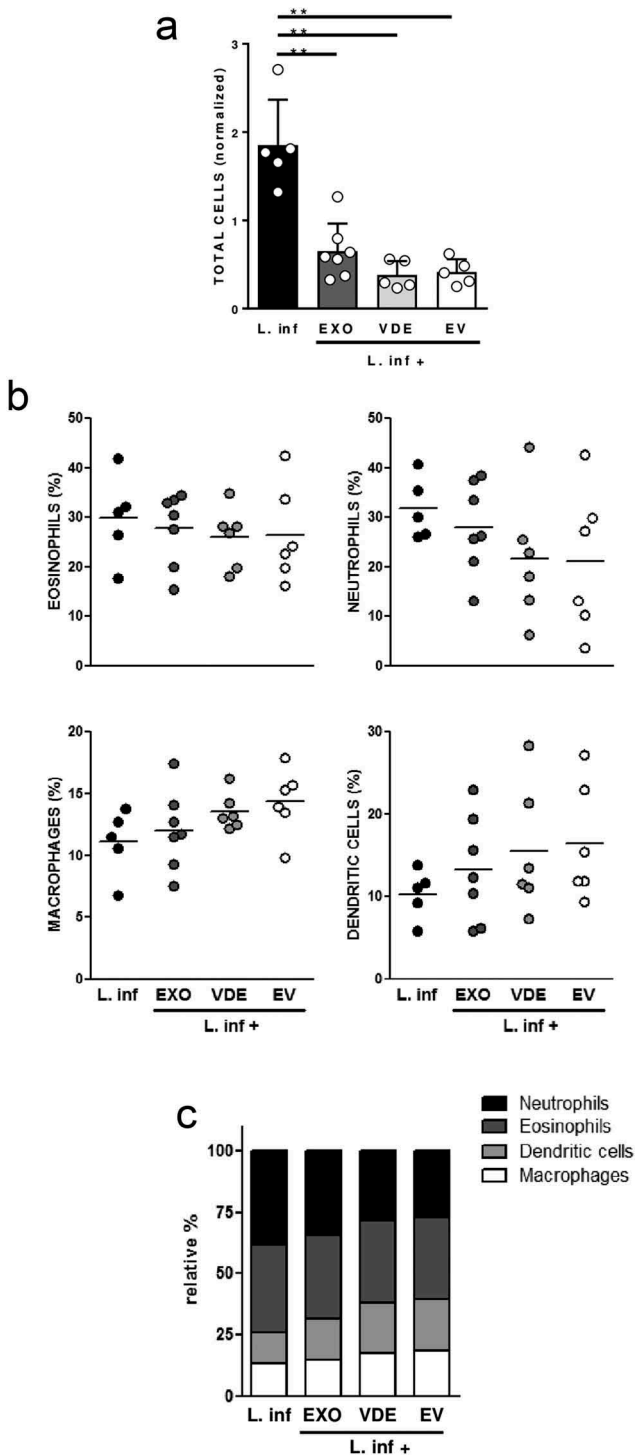


Figure 3. *Leishmania infantum* extracellular products alter the cell recruitment profile induced by the parasite. Relative number of total cells (a), frequencies of eosinophils, neutrophils, macrophages and dendritic cells (b) and relative cellular abundance (c) in mice pre-formed air pouches, 6 h after the injection of 10^6 *L. infantum* promastigotes (black), alone or together with EXO (dark grey), VDE (light grey) and EVs (white) produced by 10^7 parasites (e⁷). Each dot represents an animal; bars (a) and horizontal lines (b) indicate group means (\pm SEM) of each experimental group. One-sample *t*-test was used to assess statistical significances compared to parasites only. Significant differences are highlighted in the figure: ** $p \leq 0.01$.

CD86, CD40 and MHC-II was studied by flow cytometry as classical indicators of cell activation (Figure 4 (a)). Cell viability, determined as negative staining for 7-AAD, was similar among all the experimental conditions (S6 Fig). BMDCs in the presence of EXO and VDE presented a dose-dependent decrease of CD40 at their surface when compared to negative control ($p \leq 0.05$) while CD86 presented a trend to decrease without clear dose dependency. The EVs did not significantly modify the presence of these molecules. Similar results were observed for CD40 expression on BMM \emptyset ($p \leq 0.05$), while CD86 was not altered in these cells. The MHC-II expression at the surface of both BMDC and BMM \emptyset remained similar to the basal levels for all the conditions tested (Figure 4(a)). Using live parasites with BMDC in similar experimental settings a downregulation trend was observed for all the tested markers (S7 Fig).

The response capacity of antigen presenting cells to new stimuli is essential for coordination of the subsequent immune response. To evaluate this we used the TLR-4 ligand Lipopolysaccharide (LPS) as secondary stimuli for BMDC and BMM \emptyset cultured with EXO, VDE or EVs (Figure 4(b)). Pre-culture with EXO and EVs decreased the natural upregulation of CD86 induced by LPS (at least $p \leq 0.05$). For CD40 the same was verified, but only for BMDC (at least $p \leq 0.05$). The increase in MHC-II was strongly impaired in BMM \emptyset for all stimuli tested (at least $p \leq 0.05$) while in BMDCs it was not influenced. The endosomal TLR-3 ligand polyinosinic:polycytidylic acid (Poly I:C) was used to confirm the data obtained with LPS (S8 Fig). With this stimulus, only EXO and VDE showed ability to suppress the upregulation of the activation markers (mainly CD86 and CD40).

L. infantum extracellular products favour infection

Since parasite extracellular products can modulate DC and macrophage activation, their effect on the infection outcome was addressed in vitro. BMDC and BMM \emptyset were infected with *L. infantum* at 1:10 MOI, either alone or in combination with the lowest or the highest doses of EXO, VDE or EVs used in the previous in vitro experiments (Figure 5(a, b)). After 4 h, cells were extensively washed, the infection quantified and followed up at 24 and 48 h. Neither EXO nor its components affected the initial infection at 4 h (Figure 5(a)). However, at 48 h the presence of EXO and its fractions tendentially increased infection in BMDCs and apparently impaired parasite elimination by BMM \emptyset (Figure 5(a)).

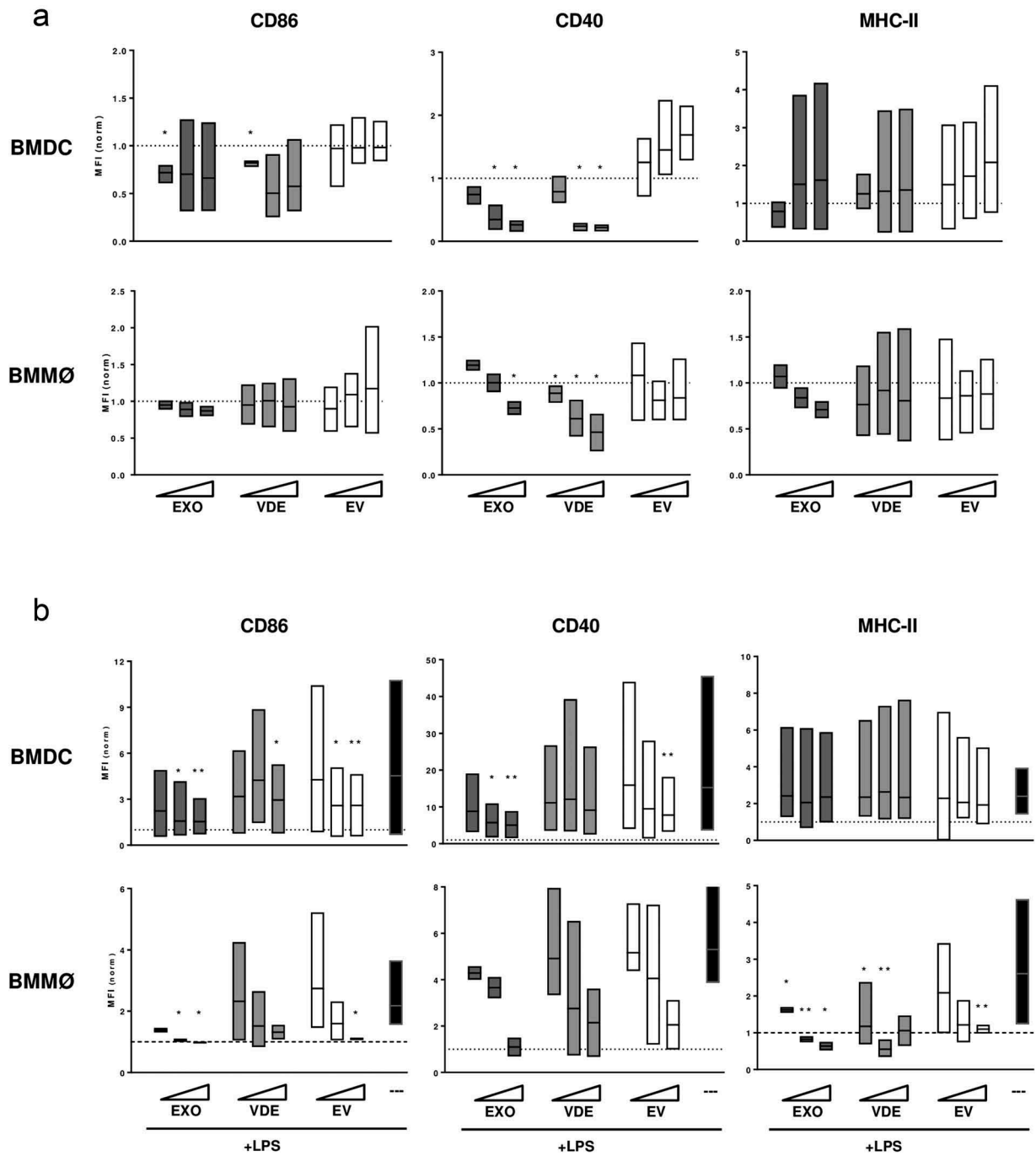


Figure 4. In vitro dose-dependent immunomodulatory effect of *L. infantum* extracellular material on BMDC and BMMØ. Normalized expression levels of CD86, CD40 and MHC-II in BMDC and BMMØ cultured for 48 h in the presence of increasing amounts of EXO (dark grey boxes), VDE (light grey boxes) and EVs (white boxes), without (a) or with (b) LPS re-stimulation 24 h after the addition of the primary stimuli. In re-stimulation assays, black boxes represent the results obtained for the positive control (LPS stimulation during the last 24 h of culture). Results are relative to the values obtained for non-stimulated cells (dotted line) and boxes illustrate the average, minimum and maximum values of three different experiments. One-sample *t*-test was used to assess statistical significances to the hypothetical negative (a) and positive (b) values. Significant differences are highlighted in the figure: * $p \leq 0.05$; ** $p \leq 0.01$.

Finally, we addressed if the presence of exogenous products in the initial inoculum could translate into a real advantage in *L. infantum* infectivity in vivo. To assess this, we used a low virulence experimental setup.

We infected BALB/c mice i.p. with 10^7 *L. infantum* that result in 50% of productive infections with readout only in spleen. Challenges were performed alone or in combination with different doses of EXO and its

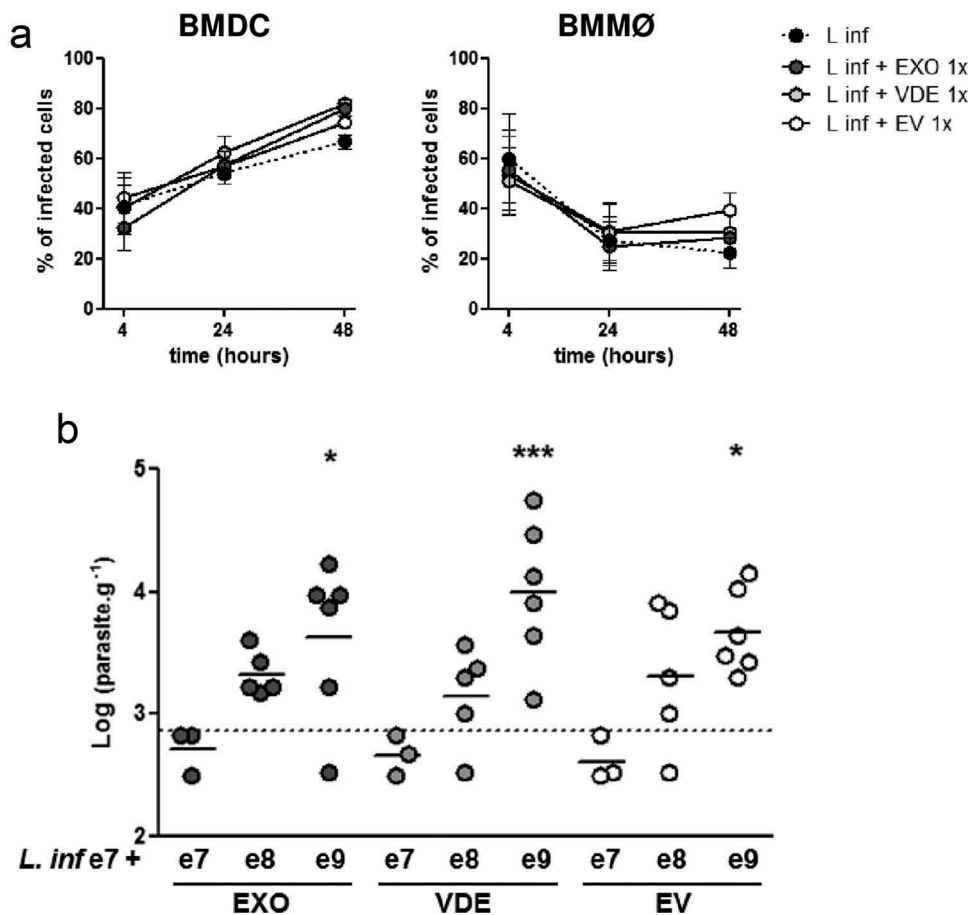


Figure 5. *Leishmania infantum* extracellular material favours infection. (a) BMDC and BMMØ were infected during 4 h with *L. infantum* promastigotes in the presence or not of *Leishmania* extracellular products. Parasites were then washed away and cells recovered or left in culture. Four, twenty-four or forty-eight hour after infection cells were cytopspined, stained by the Giemsa method and the infection analysed under the microscope. The percentage of infected cells at the different time-points is indicated. Symbols and bars represent the mean \pm SEM of three independent experiments. (b) Splenic parasite burdens of mice infected intraperitoneally with 10^7 *L. infantum* promastigotes together with EXO (dark grey dots), VDE (light grey dots) or EVs (white dots) produced by 10^7 (e^7), 10^8 (e^8) or 10^9 (e^9) parasites. Every symbol represents a mouse. Lines represent the mean of each experimental group. Statistical significance was attained comparing each group with the control group (mice infected only with 10^7 *L. infantum* promastigotes, dashed line, $n = 6$), using the One-sample *t*-test. Significant differences are highlighted in the figure: * $p \leq 0.05$, *** $p \leq 0.001$.

fractions (Figure 5(b)) and parasite burdens were determined 2 weeks after. Liver parasite burdens were below the detection limit in all the experimental settings. Notably, the parasite burden in the spleen increased in a concentration-dependent manner when *L. infantum* was co-inoculated with the extracellular products. This increase was significant for the e^9 dose of all the fractions (Figure 5(b); $p \leq 0.05$ or 0.001 for VDE).

Discussion

Several studies suggest that *Leishmania* derived EVs might have a role in the infectious process [8,13]. Still, no study evaluated the relevance of EVs in the context of other extracellular products. To understand

the effects of the secretome individual fractions is relevant when we consider the study of new virulence factors, but when the objective is to study the infectious process and translate to the natural infection, we must consider the secretome as a whole. More so relevant is this when TEM data suggests that EVs are not the most abundant component of the EXO recovered from the parasite cultures (Figure 1(a)). In fact, VDE presents higher protein levels as we shown in a previous study [9] and is suggested by the SDS-PAGE profile (S1 Fig). Therefore, it is essential to evaluate if properties reported for *Leishmania* EVs are maintained in the presence of VDE.

For the biological assays, the concept of extracellular products produced by cell number/time was used. This is an accepted approach to study EVs. Indeed, in one of

the few exosome clinical applications reported, the therapeutic unit is described as “the EV fraction prepared from supernatants of 4×10^7 mesenchymal stem cells that had been conditioned for 48 h” [34]. We considered this approach as the most relevant in our context, in opposition to the regularly used normalization by protein quantification [8]. Bearing in mind that surface interactions are essential for cross-talk between pathogens and immune system, even the equivalence between 1000 vesicles of 20 nm or 1 vesicle of 200 nm is disputable. In fact, considering protein amount proportional to the intra-vesicular volume, an EV with 200 nm diameter would have the same protein amount as 1000 vesicles of 20 nm. Notably, the measured EVs diameter variation in our samples was 10x (Figure 1(c)) translating into a volume variation of 1000x. Still, extrapolation to other biological settings due to the heterogeneous nature of EVs is always complex.

The recovered EVs are in accordance with those reported previously (Figure 1(b)) [12,33]. Moreover, distinct EVs populations with characteristic size and density were isolated suggesting a complex mixture of EVs (S2 Fig). Even so, this is still an incomplete characterization and a limitation of the study, as the need for parasite removal from the EXO by filtration eliminates particles like apoptotic bodies and large microvesicles. The recovered EVs also contained low molecular weight RNA as was already reported for other species of *Leishmania* (S3 Fig) [35]. These characteristics are in accordance with the available data on *Leishmania* EVs.

Several authors suggest that *Leishmania* derived EVs possibly function as extensions of the parasites potentiating their intrinsic capacities and contributing to immune response deactivation [13]. Here, cell recruitment associated with parasites in the air pouch model was reproduced by high doses of EXO while EVs or VDE presented dose-dependent characteristic phenotypes (Figure 2) [25]. Importantly, the selected concentrations of parasites and stimuli were used having in mind the theoretical concentration expected to be found in the site of inoculation: 500–600 parasites [36–38] deposited in the blood pool originated by the vector feeding process, which has a volume of $0.05\text{--}0.42\text{ mm}^3$ [39], giving a final average concentration of 10^7 parasites/ml. At high EXO quantities, pathogen-associated molecular patterns (PAMPs) are expected to activate endothelial cells and resident macrophages leading to neutrophils recruitment [40,41]. The few TLR activators described for *Leishmania* are expected to be part of the extracellular products. Lipophosphoglycan (LPG) is a TLR2 agonist

capable of activating mouse macrophages and human NK cells, in a MyD88-dependent manner [42–44]. Also, glycosylphosphatidylinositol, that in *T. cruzi* activates TLR2 and TLR4 [45–47], might be a PAMP present among *Leishmania* extracellular products. Even proteins might have unexpected capacities to interact with TLRs, as *L. infantum* Sir2 was demonstrated to induce the maturation of DCs in a TLR2-dependent manner with the secretion of IL-12 and TNF- α [48]. Neutrophil and eosinophil recruitment has also been associated with parasite-derived chemotactic components like the Granulocyte Chemotactic Factor described in conditioned media of several *Leishmania* species [49].

Remarkably, the lower doses of VDE tested induced less cell recruitment to the air pouch when compared to the PBS control, which was due to a lesser number of neutrophils and eosinophils (Figure 2(b)). This modulation was confirmed in the context of parasite-induced cellular recruitment in the presence of inhibitory concentrations of extracellular products (Figure 3, S5 Fig). Lipid mediators like lipoxin A4 are known to be associated with the resolution of inflammation, inhibiting neutrophil chemotaxis and promoting non-inflammatory macrophage recruitment [41,50]. Pathogens like *Pseudomonas aeruginosa* and *Toxoplasma gondii* can induce local lipoxin production [51,52]. Intriguingly, *Leishmania* was shown to release a molecule described to interact with the lipoxin A4 receptor leading to increased survival of the parasites inside macrophages [53]. The negative immune regulation observed can also be justified by an adaptation of the “trojan horse” theory [49,54]. Exosomes and apoptotic bodies found in the EVs preparations are known to contain phosphatidylserine exposed at their surface [55,56], a known “eat me signal”, with the potential to modulate cell recruitment and promote the generation of an anti-inflammatory environment [57–59], beneficial for parasite persistence.

Dendritic cells were the only cell type that presented a fraction specific recruitment in response to VDE and EVs (Figure 2). This phenotype was not observed for EXO, suggesting that the recruitment might be masked by its inflammatory profile in the higher doses tested. Significantly, the recruitment of DCs was retained when EVs or VDE were co-inoculated with parasites, suggesting that both the nature and the dose of the extracellular products might modulate the parasite associated cellular recruitment. Moreover, DCs present upon *Leishmania* and extracellular products inoculation in the air pouch were not activated (S4 Fig). The downregulation of activations markers by parasites was described by several authors and is thought to be an essential component of the *Leishmania* immunomodulatory arsenal [5,26].

Ultimately the DCs recruitment to the infection site and their subsequent deactivation might lead to an adaptive immune response delay, giving the parasite enough time to either escape the inoculation site inside a permissive phagocytic cell or create a privileged niche that enables a silent progression of infection [60,61].

Intracellularly these parasites can dampen the immune response by direct modulation of host signaling [10,11]. Here we show that EXO and its components, in the dose range tested, presented distinct capacities to alter the expression of CD40, CD86 and MHCII *in vitro*, being VDE the most capable fraction (Figure 4(a)). This specific effect was expected as VDE is highly enriched in several known immunomodulatory proteins. GP63, a metalloprotease that may cleave cytosolic host proteins like tyrosine phosphatases [62] and serine/threonine kinase (mTOR) [11], contributing to macrophage anergy [62,63], was shown by our group to be particularly abundant in the exoproteome [9]. Furthermore, elongation factor-1 α , another major component of *Leishmania* exoproteome, was shown to deactivate macrophage functions by triggering the Src homology 2 domain in tyrosine phosphatase-1 [17]. Also, LPG was shown to attenuate multiple macrophage functions including phagosome maturation, oxygen radical formation and cell signalling through effects on protein kinase C [64–66]. The cellular alterations induced by extracellular products were not limited to the downregulation of activation markers. Interestingly, although EVs did not alter the basal phenotype of DCs and macrophages, they presented an equivalent potency to VDE in dampening the response to the TLR4 agonist LPS (Figure 4(b)). It is important to note that this effect was not evident when re-stimulation was performed with the TLR3 agonist Poly I:C (Figure S8). The cellular localization of the TLR (surface for TLR4 or endosomes for TLR3) might be important for these distinct phenotypes as free molecules present in EXO, or VDE might more easily access intracellular compartments. The importance of cellular alterations induced by exogenous products goes beyond the obvious effect on infected cells, as their presence in the initial inoculum might also contribute to non-infected cells deactivation, preventing the formation of a zonal NO gradient, described to be important for parasite clearance [67].

Using *in vitro* infection models no differences in parasite uptake were observed, suggesting that the presence of exogenous products in the initial inoculum neither stimulates nor hinders parasite phagocytosis (Figure 5(a, b)). Still, there was a modest increase of infection at the latter time points suggesting that the exogenous products might

potentiate infectivity. The absence of significance might be justified by the intrinsic capacity of the parasite to induce modulation of infected cell's responses (Fig S7). In fact, in our *in vivo* infection model, the presence of exogenous products in the inoculum potentiated the infection in a dose-dependent manner (Figure 5(c)), suggesting that parasite-secreted components can play a role in infection establishment. Interestingly, when 10^8 parasites were used in the same context no advantage was observed, suggesting that in this case parasite numbers might have been so overwhelming that no further biological benefit was granted by EXO or its components (data not shown).

As far as we are concerned, we report for the first time that the outcome of the interactions between parasite exogenous products and the immune system is not only influenced by their nature but also by their quantity, suggesting that the event of a productive infection would have to include a specific combination of parasite, parasite-derived material and also sand fly saliva-derived components (saliva and microbiome). Interestingly, the described exoproteome dual capacity of apparent inflammation induction or dampening might be essential for distinct aspects of the parasite life cycle, such as the need to recruit susceptible cells and/or to prevent their activation. In the moment of transmission, the relevance of EVs immunomodulatory potential has always to be considered in the context of the whole *Leishmania* secretome. However, the importance of EVs alone might be more relevant for the intracellular stage of the parasite (which resides and replicates within the acidic host-cell phagolysosome) as these will probably be key for the delivery of parasite-derived components to the cell cytoplasm that could contribute to the manipulation of the host cell, subject we are now focusing on.

Acknowledgments

The authors would like to thank Parolab for making available the NanoSight (Malvern Instruments Ltd, UK).

Data availability

All relevant data are within the article and its Supporting Information files.

Disclosure statement

No potential conflict of interest was reported by the authors.

Funding

This article is a result of the project NORTE-01-0145-FEDER-000012, supported by Norte Portugal Regional Operational

Programme (NORTE 2020), under the PORTUGAL 2020 Partnership Agreement, through the European Regional Development Fund (ERDF). This work was also funded by FEDER through the Operational Competitiveness Programme – COMPETE and by National Funds through FCT – Fundação para a Ciência e a Tecnologia under the project FCOMP-01-0124-FEDER-019648 (PTDC/BIA-MIC/118644/2010). PC was supported by Foundation for Science and Technology (FCT), Portugal, through the individual grant SFRH/BD/121252/2016.

References

- [1] Naderer T, McConville MJ. Intracellular growth and pathogenesis of *Leishmania* parasites. *Essays Biochem.* **2011**;51:81–95. bse0510081 [pii]. PubMed PMID: 22023443; eng.
- [2] WHO. *Leishmaniasis, Fact sheet N°375* 2014. [cited 2015 Jan 19].
- [3] Cecilio P, Oliveira F, Cordeiro-da-Silva A. Vaccines for human leishmaniasis: where do we stand and what is still missing? In: Afrin F, editor. *Leishmaniasis as re-emerging diseases*. Rijeka: IntechOpen; **2018**: 59–93.
- [4] Loria-Cervera EN, Andrade-Narvaez FJ. Animal models for the study of leishmaniasis immunology. *Rev Inst Med Trop Sao Paulo.* **2014** Jan–Feb;56(1): 1–11.
- [5] Cecilio P, Perez-Cabezas B, Santarem N, et al. Deception and manipulation: the arms of leishmania, a successful parasite. *Front Immunol.* **2014**;5:480. PubMed PMID: 25368612; PubMed Central PMCID: PMC4202772. eng
- [6] Teixeira C, Gomes R, Oliveira F, et al. Characterization of the early inflammatory infiltrate at the feeding site of infected sand flies in mice protected from vector-transmitted *Leishmania major* by exposure to uninfected bites. *PLoS Negl Trop Dis.* **2014** Apr;8(4): e2781. PubMed PMID: 24762408; PubMed Central PMCID: PMC43998922.
- [7] Rogers ME, Corware K, Muller I, et al. *Leishmania infantum* proteophosphoglycans regurgitated by the bite of its natural sand fly vector, *Lutzomyia longipalpis*, promote parasite establishment in mouse skin and skin-distant tissues. *Microbes Infect.* **2010** Oct;12(11):875–879. PubMed PMID: 20561596; eng.
- [8] Atayde VD, Aslan H, Townsend S, et al. Exosome secretion by the parasitic protozoan leishmania within the sand fly midgut. *Cell Rep.* **2015** Nov 3;13(5):957–967. PubMed PMID: 26565909; PubMed Central PMCID: PMC4644496. eng.
- [9] Santarem N, Racine G, Silvestre R, et al. Exoproteome dynamics in *Leishmania infantum*. *J Proteomics.* **2013** Jun 12;84:106–118. PubMed PMID: 23558030; eng.
- [10] Halle M, Gomez MA, Stuible M, et al. The *Leishmania* surface protease GP63 cleaves multiple intracellular proteins and actively participates in p38 mitogen-activated protein kinase inactivation. *J Biol Chem.* **2009** Mar 13;284(11):6893–6908. PubMed PMID: 19064994; PubMed Central PMCID: PMC2652307. eng.
- [11] Jaramillo M, Gomez MA, Larsson O, et al. *Leishmania* repression of host translation through mTOR cleavage is required for parasite survival and infection. *Cell Host Microbe.* **2011** Apr 21;9(4):331–341. PubMed PMID: 21501832; eng.
- [12] Silverman JM, Clos J, de'Oliveira CC, et al. An exosome-based secretion pathway is responsible for protein export from *Leishmania* and communication with macrophages. *J Cell Sci.* **2010** Mar 15;123(Pt 6):842–852. PubMed PMID: 20159964; eng.
- [13] Silverman JM, Reiner NE. *Leishmania* exosomes deliver preemptive strikes to create an environment permissive for early infection. *Front Cell Infect Microbiol.* **2011**;1:26. PubMed PMID: 22919591; PubMed Central PMCID: PMC3417360. eng
- [14] Atayde VD, Hassani K, Da Silva Lira Filho A, et al. *Leishmania* exosomes and other virulence factors: impact on innate immune response and macrophage functions. *Cell Immunol.* **2016** Nov;309:7–18. PubMed PMID: 27499212.
- [15] Marshall S, Kelly PH, Bk S, et al. Extracellular release of virulence factor major surface protease via exosomes in *Leishmania infantum* promastigotes. *Parasit Vectors.* **2018** Jun 19;11(1):355. PubMed PMID: 29921321; PubMed Central PMCID: PMC6006689.
- [16] Carvalho LP, Passos S, Dutra WO, et al. Effect of LACK and KMP11 on IFN-gamma production by peripheral blood mononuclear cells from cutaneous and mucosal leishmaniasis patients. *Scand J Immunol.* **2005** Apr;61(4):337–342. PubMed PMID: 15853916; eng.
- [17] Nandan D, Yi T, Lopez M, et al. *Leishmania* EF-1alpha activates the Src homology 2 domain containing tyrosine phosphatase SHP-1 leading to macrophage deactivation. *J Biol Chem.* **2002** Dec 20;277(51):50190–50197. PubMed PMID: 12384497; eng.
- [18] Nandan D, Tran T, Trinh E, et al. Identification of leishmania fructose-1,6-bisphosphate aldolase as a novel activator of host macrophage Src homology 2 domain containing protein tyrosine phosphatase SHP-1. *Biochem Biophys Res Commun.* **2007** Dec 21;364(3):601–607. PubMed PMID: 18028878; eng.
- [19] Yanez-Mo M, Siljander PR, Andreu Z, et al. Biological properties of extracellular vesicles and their physiological functions. *J Extracell Vesicles.* **2015**;4:27066. PubMed PMID: 25979354; PubMed Central PMCID: PMC4433489. eng
- [20] Coakley G, Maizels RM, Buck AH. Exosomes and other extracellular vesicles: the new communicators in parasite infections. *Trends Parasitol.* **2015** Oct;31(10):477–489. PubMed PMID: 26433251; PubMed Central PMCID: PMC4685040
- [21] Santarem N, Cunha J, Silvestre R, et al. The impact of distinct culture media in *Leishmania infantum* biology and infectivity. *Parasitology.* **2014** Feb;141(2):192–205. PubMed PMID: 24007671; eng.
- [22] Consortium E-T, Van Deun J, Mestdagh P, et al. EV-TRACK: transparent reporting and centralizing knowledge in extracellular vesicle research. *Nat Methods.* **2017** Feb 28;14(3):228–232. PubMed PMID: 28245209.
- [23] Edwards JC, Sedgwick AD, Willoughby DA. The formation of a structure with the features of synovial lining by subcutaneous injection of air: an in vivo tissue culture system. *J Pathol.* **1981** Jun;134(2):147–156. PubMed PMID: 7019400.

- [24] Matte C, Marquis JF, Blanchette J, et al. Peroxovanadium-mediated protection against murine leishmaniasis: role of the modulation of nitric oxide. *Eur J Immunol.* **2000** Sep;30(9):2555–2564. PubMed PMID: 11009089.
- [25] Matte C, Olivier M. Leishmania-induced cellular recruitment during the early inflammatory response: modulation of proinflammatory mediators. *J Infect Dis.* **2002** Mar 1;185(5):673–681. PubMed PMID: 11865425; eng.
- [26] Bm N, Silvestre R, Resende M, et al. Activation of phosphatidylinositol 3-kinase/Akt and impairment of nuclear factor-kappaB: molecular mechanisms behind the arrested maturation/activation state of *Leishmania infantum*-infected dendritic cells. *Am J Pathol.* **2010** Dec;177(6):2898–2911. PubMed PMID: 21037075; PubMed Central PMCID: PMC2993270. eng.
- [27] Faria J, Loureiro I, Santarem N, et al. Disclosing the essentiality of ribose-5-phosphate isomerase B in *Trypanosomatids*. *Sci Rep.* **2016**;6:26937. PubMed PMID: 27230471; PubMed Central PMCID: PMC4882579. eng.
- [28] Cunha J, Carrillo E, Sanchez C, et al. Characterization of the biology and infectivity of *Leishmania infantum* viscerotropic and dermatotropic strains isolated from HIV+ and HIV- patients in the murine model of visceral leishmaniasis. *Parasit Vectors.* **2013**;6:122. PubMed PMID: 23622683; PubMed Central PMCID: PMC3649922
- [29] Rose S, Misharin A, Perlman H. A novel Ly6C/Ly6G-based strategy to analyze the mouse splenic myeloid compartment. *Cytometry A.* **2012** Apr;81(4):343–350. PubMed PMID: 22213571; PubMed Central PMCID: PMC3987771
- [30] Perez-Cabezas B, Cecilio P, Robalo AL, et al. Interleukin-27 early impacts *Leishmania infantum* infection in mice and correlates with active visceral disease in humans. *Front Immunol.* **2016**;7:478. PubMed PMID: 27867384; PubMed Central PMCID: PMC5095612. eng
- [31] Silvestre R, Cordeiro-Da-Silva A, Santarem N, et al. SIR2-deficient *Leishmania infantum* induces a defined IFN-gamma/IL-10 pattern that correlates with protection. *J Immunol.* **2007** Sep 1;179(5):3161–3170. PubMed PMID: 17709531.
- [32] Mathivanan S, Ji H, Rj S. Exosomes: extracellular organelles important in intercellular communication. *J Proteomics.* **2010** Sep 10;73(10):1907–1920. S1874-3919(10)00184-3 [pii]. PubMed PMID: 20601276; eng.
- [33] Hassani K, Shio MT, Martel C, et al. Absence of metalloprotease GP63 alters the protein content of leishmania exosomes. *PLoS One.* **2014**;9(4):e95007. PubMed PMID: 24736445; PubMed Central PMCID: PMC3988155. eng
- [34] Kordelas L, Rebmann V, Ak L, et al. MSC-derived exosomes: a novel tool to treat therapy-refractory graft-versus-host disease. *Leukemia.* **2014** Apr;28(4):970–973. PubMed PMID: 24445866; eng.
- [35] Lambert U, Oviedo Ovando ME, Vasconcelos EJ, et al. Small RNAs derived from tRNAs and rRNAs are highly enriched in exosomes from both old and new world *Leishmania* providing evidence for conserved exosomal RNA packaging. *BMC Genomics.* **2015**;16:151. PubMed PMID: 25764986; PubMed Central PMCID: PMC4352550. eng
- [36] Kimblin N, Peters N, Debrabant A, et al. Quantification of the infectious dose of *Leishmania major* transmitted to the skin by single sand flies. *Proc Natl Acad Sci U S A.* **2008** Jul 22;105(29):10125–10130. PubMed PMID: 18626016; PubMed Central PMCID: PMC2481378. eng.
- [37] Maia C, Seblova V, Sadlova J, et al. Experimental transmission of *Leishmania infantum* by two major vectors: a comparison between a viscerotropic and a dermatotropic strain. *PLoS Negl Trop Dis.* **2011** Jun;5(6):e1181. PubMed PMID: 21695108; PubMed Central PMCID: PMC3114756.
- [38] Stamper LW, Patrick RL, Fay MP, et al. Infection parameters in the sand fly vector that predict transmission of *Leishmania major*. *PLoS Negl Trop Dis.* **2011** Aug;5(8):e1288. PubMed PMID: 21886852; PubMed Central PMCID: PMC3160291.
- [39] Doehl JSP, Bright Z, Dey S, et al. Skin parasite landscape determines host infectiousness in visceral leishmaniasis. *Nat Commun.* **2017** Jul 5;8(1):57. PubMed PMID: 28680146; PubMed Central PMCID: PMC5498584.
- [40] Mogensen TH. Pathogen recognition and inflammatory signaling in innate immune defenses. *Clin Microbiol Rev.* **2009** Apr;22(2): 240–273. Table of Contents.
- [41] Kolaczowska E, Kubes P. Neutrophil recruitment and function in health and inflammation. *Nat Rev Immunol.* **2013** Mar;13(3): 159–175.
- [42] de Veer MJ, Curtis JM, Baldwin TM, et al. MyD88 is essential for clearance of *Leishmania major*: possible role for lipophosphoglycan and toll-like receptor 2 signaling. *Eur J Immunol.* **2003** Oct;33(10):2822–2831. PubMed PMID: 14515266; eng.
- [43] Becker I, Salaiza N, Aguirre M, et al. *Leishmania* lipophosphoglycan (LPG) activates NK cells through toll-like receptor-2. *Mol Biochem Parasitol.* **2003** Aug 31;130(2):65–74. PubMed PMID: 12946842; eng.
- [44] Kavooosi G, Ardestani SK, Kariminia A, et al. *Leishmania major* lipophosphoglycan: discrepancy in toll-like receptor signaling. *Exp Parasitol.* **2010** Feb;124(2):214–218. PubMed PMID: 19769970; eng.
- [45] Campos MA, Almeida IC, Takeuchi O, et al. Activation of Toll-like receptor-2 by glycosylphosphatidylinositol anchors from a protozoan parasite. *J Immunol.* **2001** Jul 1;167(1):416–423. PubMed PMID: 11418678; eng.
- [46] Almeida IC, Gazzinelli RT. Proinflammatory activity of glycosylphosphatidylinositol anchors derived from *Trypanosoma cruzi*: structural and functional analyses. *J Leukoc Biol.* **2001** Oct;70(4):467–477. PubMed PMID: 11590183; eng
- [47] Almeida IC, Camargo MM, Procopio DO, et al. Highly purified glycosylphosphatidylinositols from *Trypanosoma cruzi* are potent proinflammatory agents. *Embo J.* **2000** Apr 3;19(7):1476–1485. PubMed PMID: 10747016; PubMed Central PMCID: PMC310217. eng.
- [48] Silvestre R, Silva AM, Cordeiro-da-Silva A, et al. The contribution of Toll-like receptor 2 to the innate recognition of a *Leishmania infantum* silent information regulator 2 protein. *Immunology.* **2009** Dec;128

- (4):484–499. PubMed PMID: 19930041; PubMed Central PMCID: PMC2792133. eng.
- [49] van Zandbergen G, Hermann N, Laufs H, et al. Leishmania promastigotes release a granulocyte chemoattractant factor and induce interleukin-8 release but inhibit gamma interferon-inducible protein 10 production by neutrophil granulocytes. *Infect Immun*. 2002 Aug;70(8):4177–4184. PubMed PMID: 12117926; PubMed Central PMCID: PMC128123. eng.
- [50] Serhan CN, Chiang N, Van Dyke TE. Resolving inflammation: dual anti-inflammatory and pro-resolution lipid mediators. *Nat Rev Immunol*. 2008 May;8(5):349–361. PubMed PMID: 18437155; PubMed Central PMCID: PMC2744593. eng. .
- [51] Vance RE, Hong S, Gronert K, et al. The opportunistic pathogen *Pseudomonas aeruginosa* carries a secretable arachidonate 15-lipoxygenase. *Proc Natl Acad Sci U S A*. 2004 Feb 17;101(7):2135–2139. PubMed PMID: 14766977; PubMed Central PMCID: PMC357064. eng.
- [52] Bannenberg GL, Aliberti J, Hong S, et al. Exogenous pathogen and plant 15-lipoxygenase initiate endogenous lipoxin A4 biosynthesis. *J Exp Med*. 2004 Feb 16;199(4):515–523. PubMed PMID: 14970178; PubMed Central PMCID: PMC2211821. eng.
- [53] Wenzel A, Van Zandbergen G. Lipoxin A4 receptor dependent leishmania infection. *Autoimmunity*. 2009 May;42(4):331–333. PubMed PMID: 19811292; eng
- [54] van Zandbergen G, Bollinger A, Wenzel A, et al. Leishmania disease development depends on the presence of apoptotic promastigotes in the virulent inoculum. *Proc Natl Acad Sci U S A*. 2006 Sep 12;103(37):13837–13842. PubMed PMID: 16945916; PubMed Central PMCID: PMC1564231.
- [55] Gyorgy B, Szabo TG, Pasztoi M, et al. Membrane vesicles, current state-of-the-art: emerging role of extracellular vesicles. *Cell Mol Life Sci*. 2011 Aug;68(16):2667–2688. PubMed PMID: 21560073; PubMed Central PMCID: PMC3142546.
- [56] Chaput N, Thery C. Exosomes: immune properties and potential clinical implementations. *Semin Immunopathol*. 2011 Sep;33(5):419–440. PubMed PMID: 21174094
- [57] Birge RB, Boeltz S, Kumar S, et al. Phosphatidylserine is a global immunosuppressive signal in efferocytosis, infectious disease, and cancer. *Cell Death Differ*. 2016 Jun;23(6):962–978. PubMed PMID: 26915293; PubMed Central PMCID: PMC4987730.
- [58] Hochreiter-Hufford A, Ravichandran KS. Clearing the dead: apoptotic cell sensing, recognition, engulfment, and digestion. *Cold Spring Harb Perspect Biol*. 2013 Jan 01;5(1):a008748. PubMed PMID: 23284042; PubMed Central PMCID: PMC3579390.
- [59] Park SY, Kim IS. Engulfment signals and the phagocytic machinery for apoptotic cell clearance. *Exp Mol Med*. 2017 May 12;49(5):e331. PubMed PMID: 28496201; PubMed Central PMCID: PMC5454446.
- [60] Santarem N, Silvestre R, Tavares J, et al. Immune response regulation by leishmania secreted and nonsecreted antigens. *J Biomed Biotechnol*. 2007;2007(6):85154. PubMed PMID: 17710243; PubMed Central PMCID: PMC1940321. eng
- [61] Chang KP, Reed SG, McGwire BS, et al. Leishmania model for microbial virulence: the relevance of parasite multiplication and pathoantigenicity. *Acta Trop*. 2003 Mar;85(3):375–390. S0001706X02002383 [pii]. PubMed PMID: 12659975; eng.
- [62] Gomez MA, Contreras I, Halle M, et al. Leishmania GP63 alters host signaling through cleavage-activated protein tyrosine phosphatases. *Sci Signal*. 2009;2(90):ra58. PubMed PMID: 19797268; eng.
- [63] Contreras I, Gomez MA, Nguyen O, et al. Leishmania-induced inactivation of the macrophage transcription factor AP-1 is mediated by the parasite metalloprotease GP63. *PLoS Pathog*. 2010;6(10):e1001148. PubMed PMID: 20976196; PubMed Central PMCID: PMC2954837. eng
- [64] Descoteaux A, Matlashewski G, Turco SJ. Inhibition of macrophage protein kinase C-mediated protein phosphorylation by *Leishmania donovani* lipophosphoglycan. *J Immunol*. 1992 Nov 1;149(9):3008–3015. PubMed PMID: 1383336; eng
- [65] Lodge R, Descoteaux A. Modulation of phagolysosome biogenesis by the lipophosphoglycan of *Leishmania*. *Clin Immunol*. 2005 Mar;114(3): 256–265.
- [66] Dermine JF, Goyette G, Houde M, et al. *Leishmania donovani* lipophosphoglycan disrupts phagosome microdomains in J774 macrophages. *Cell Microbiol*. 2005 Sep;7(9):1263–1270. PubMed PMID: 16098214; eng.
- [67] Olekhovitch R, Ryffel B, Muller AJ, et al. Collective nitric oxide production provides tissue-wide immunity during *Leishmania* infection. *J Clin Invest*. 2014 Apr;124(4):1711–1722. PubMed PMID: 24614106; PubMed Central PMCID: PMC3973105. eng.